

Shrinkage Characteristics of Heat-tacked GCL Seams

R. Kerry Rowe¹, Laura Bostwick¹, Richard Thiel²

¹ GeoEngineering Centre at Queen's-RMC, Department of Civil Engineering, Queen's University, Kingston, ON, Canada, K7L 3N6, 613-533-6933 email kerry@civil.queensu.ca

² Vector Engineering, 143E Spring Hill Dr., Grass Valley, CA 95945, USA, phone 530-272-2448, fax 530-272-8533, email richard@rthiel.com

ABSTRACT

The behavior of heat-tacked GCL seams under cyclic wetting and drying is examined. It is shown that the transverse shrinkage behavior of heat-tacked seams was similar to that observed in previous shrinkage tests performed on unseamed GCL. It is shown that the heat-tacked seam has strength comparable to the GCL adjacent to the seam and hence it is likely the strength of the GCL itself that will govern failure of the GCL in applications where there can be significant shrinkage. The strength of the heat-tacked seam subjected to 40 wet-dry cycles was at least as high as that of virgin heat-tacked samples, suggesting that 40 wet-dry cycles did not weaken the heat-tacked seam. After 40 cycles, the samples remained heat-tacked, suggesting the technique has promise as one method of preventing panel shrinkage for GCLs highly susceptible to shrinkage. It is noted that these tests are small-scale laboratory tests, under idealized conditions, and that the behavior in the field may differ due to more extreme conditions that may occur in the field and due to the greater amount of material between seams available to shrink and hence induce forces in the heat-tacked GCL seam.

Keywords: GCL, shrinkage, seam strength

1. Introduction

Geosynthetic clay liners (GCLs) have gained wide acceptance for use as part of composite liner systems (Rowe et al. 2004, Brachman and Gudina 2008, Gassner 2009) and have been shown to give rise to less leakage than systems involving the use of a compacted clay liner (Rowe 2005). However this good performance is predicated on the GCL being continuous beneath the geomembrane. Separation of the GCL panels beneath the geomembrane would have a serious negative impact on the performance of the composite liner.

The potential for GCL panel separation due to shrinkage of geosynthetic clay liners (GCLs) covered by a geomembrane (GM) and left exposed (i.e. with no overlying cover soil), first highlighted by Thiel and Richardson (2005), was emphasized by five reported cases where GCL panels, originally overlapped by 150 mm, had opened up leaving separations between GCL panels of between 200 and 1200 mm after periods of exposure of between 2 and 36 months (Koerner & Koerner 2005a, 2005b; Thiel et al. 2006). Laboratory studies (Thiel et al. 2006; Bostwick et al. 2007, 2008, Rowe et al. 2009) have demonstrated that shrinkage of up to 23% could be induced in the laboratory by the application of cyclic wetting and drying. The laboratory work indicated that shrinkage is related to both the number and intensity of wet-dry cycles. Thus, amongst other things, panel shrinkage may be related to the period of exposure since, other things being equal, the number of shrinkage cycles will be greater the longer the composite liner remains uncovered. The laboratory research also demonstrated that some products were more susceptible to shrinkage than others as summarized in Table 1.

The risk of shrinkage causing a separation of panels is relatively high for exposed composite liners where the GCL overlap is the traditional 150mm. This risk of panel separation can be considerably reduced by overlapping the panels by 300 mm *and* placing cover soil on the GM as quickly as possible (within 30 days). However in some large field applications, there is significant cost associated with increasing the amount of GCL in order to double the panel overlap. Also in some cases it may be impractical to cover all of the composite liner within less than 30 days. For these situations an alternative approach that would minimize the potential for the reduction or total loss of the overlap would be highly desirable.

A novel field approach to addressing the concern regarding separation of panels of GCL3 and GCL4 when used as part of a composite liner for a large (60ha) heap leach pad at the Carlota Mine in Arizona, USA (latitude 33°N) was recently proposed by Thiel and Thiel (2009). The composite liner was constructed on a subgrade of a gravelly, silty sand of low plasticity that is subject to rapid drying in the local climate. The as-compacted subgrade moisture content was 10% to 12% but due to the arid climate the moisture content decreased with depth. Depending on the proximity of the time of installation to rainfall events and the location within the leach pad the subgrade moisture content may have varied between 5% and 20% when the GCL was placed. GCL4 was used on slopes where its enhanced shear strength (compared to GCL3) was needed, even though this particular GCL experienced the greatest shrinkage in laboratory tests and in field cases where loss of overlap had been observed (Table 1). Since GCL3 was slightly less expensive, it was used in flatter areas where shear strength demands were not as great. The 150 mm GCL panel overlaps were heat-tacked using a flame torch and then

pressed together using light pressure from a sand-filled bag (Figure 1). The geomembrane was placed over the GCL on same day but it was often left un-ballasted for 60 days or more before cover soil was placed over the composite liner. Prior to covering, the CQA firm cut holes through the geomembrane to exhume the GCL in areas that had been uncovered for more than 60 days to verify that the GCL overlaps had remained intact. Between the months of February and June, the exhumations were performed at mid-slope in six separate areas. The ambient temperature during this period of exhumations varied from below 0°C to above 32°C. Both GCL3 and GCL4 were evaluated and in every case examined there was no evidence of any GCL shrinkage and the heat-tacked GCL seam was intact.

The use of heat-tacking instead of increasing the panel overlap to 300 mm to address concerns regarding possible panel overlap separation provided significant savings at the site. However given the sensitivity of panel shrinkage and separation of the local environmental conditions and the nature and moisture content of the subgrade, it is not known whether the lack of observable shrinkage and the lack of separation at this site was fortuitous (i.e. if no significant shrinkage would have occurred in any event) or because the heat-tacking of the overlaps prevented panel separation. The question has been raised as to whether the heat-tacked GCL panel overlaps had sufficient strength to withstand shrinkage of the GCL. The objective of this paper is to provide some initial insight into this question based on a series of laboratory pan shrinkage tests conducted using heat-tacked GCL seams from the Carlota Mine. Initial results for one such seam were reported by Rowe et al. (2009). This present paper builds on the earlier conference

paper (Rowe et al. 2009) and includes both the results contained in the earlier paper as well as results from a number of other tests that were subsequently conducted.

2. Laboratory Testing Program

2.1 Materials

To investigate the potential of heat-tacking in preventing GCL panel shrinkage, a laboratory testing program was initiated. Samples of a GCL with a nonwoven carrier geotextile, a nonwoven cover geotextile and a coarse granular bentonite, denoted as GCL4 (Table 1), were tested. The GCL samples had been heat-tacked in the field at the Carlota Copper Mine in Arizona. The GCL samples were subjected to numerous wetting and drying cycles. This type of GCL had previously been noted for its high shrinkage in both laboratory tests (Thiel 2006, Bostwick et al. 2008) and field installations (Thiel and Richardson 2005).

Three 420mm x 225mm samples were tested, with the seamed portion (measuring approximately 150mm) located in the centre of the sample. Excess material was trimmed so that only the heat-tacked portion of the seam remained. The edges of the sample were then wrapped in moisture barrier tape, to prevent loss of bentonite and moisture from the edges of the sample. The initial properties of each sample were recorded, and are summarized in Table 1. Preliminary results from sample “A” were previously reported by Rowe et al. (2009).

2.2 Test Setup

The test setup was based upon earlier laboratory studies of GCL shrinkage (Thiel et al. 2006, Bostwick et al. 2008), scaled down to accommodate smaller samples. For

these particular tests, a 420mm x 320mm aluminum baking pan was drilled along each side with 7mm holes, which acted as control markers for later photogrammetry analysis. The samples were then attached to the pans by means of a 25mm-wide, 300mm-long C-clamp. This restraint allowed forces in both the transverse and longitudinal directions to develop, putting the sample into tension.

After the samples were attached to the pan, the “area of interest” on each sample was defined, in order to reduce edge effects. A border was drawn approximately 25mm from sample edges and from clamps, leaving an area measuring 175mm x 300 mm. The aspect ratio of this “area of interest”, 1.6, is approximately the same as that used in previous, larger pan-style tests. Grid lines were drawn at the middle and quarter points of each sample; these lines were used for later hand measurements (the results of which are included in Bostwick (2009)). An example of a final pan set-up is shown in Figure 2.

2.3 Testing Procedure

Following the assembly of each pan, initial photographs were taken to use as a baseline for comparison. In addition, initial hand measurements were taken at each of the 5 transverse grid lines (Figure 2). Each sample was then wet, by means of a commercial garden sprayer, with an amount of water roughly equal to 60% of the dry unit mass of the sample. This brought each sample to an approximate moisture content of 66% on the first cycle, and 61% on each subsequent cycle. The amount of water added to each pan, as well as the target moisture content, is summarized in Table 2. When wetting, more water was added to the seamed portion of the sample to ensure that the bentonite in the entire sample was reasonably evenly hydrated.

Following wetting, the samples were left to hydrate in a 20°C temperature-controlled room for approximately 7 hours, to allow for equilibrium of the moisture content throughout the GCL. Each sample was placed in an individual envelope constructed of moisture-barrier plastic (Polytarp Supersix PE), to prevent loss of moisture to the atmosphere. After the hydration period, pans were placed in a 60°C oven for approximately 16 hours. This wetting and drying cycle is identical to that used previously in pan-style shrinkage tests by Bostwick et al. (2008) and Rowe et al. (2009). The process was repeated until each sample had undergone forty cycles.

3. Definition and Measurement of GCL Strain

Strain across the seamed GCL was calculated in two directions – the transverse direction (which corresponds to the machine direction off the roll), and the longitudinal direction (which corresponds to the cross direction off the roll). These directions are shown on Figure 2.

During testing, shrinkage strain was calculated using hand measurements taken, to the nearest mm, at each of the five transverse lines drawn on the sample. Strain was calculated at the end of each wetting and drying cycle, and an approximate indication of how the sample was behaving as the testing continued.

For the final analysis, greater precision was required. Therefore, a code known as geoPIV (Particle Image Velocimetry - White et al. 2003) was used to calculate strains. Throughout the testing process, photographs were taken of each sample using a 10MP digital SLR camera; photographs were taken at the end of both the shrinkage and swelling portions of each cycle. By comparing the positions of user-created virtual “patches” from one image to the next, an accurate value of strain could be obtained. An

example of these virtual patches is shown in Figure 3, where a series of overlapping 128-pixel patches were drawn along the longitudinal border lines.

GeoPIV is capable of calculating strains to an accuracy of 0.1 pixels (White et al. 2003); the images used for analysis in this paper have an approximate resolution of 0.17 mm per pixel, resulting in an accuracy of roughly 0.017mm. The accuracy of strain measurements is dependant upon the gage distance measured; for strain calculations across the entire transverse gage distance of the sample (175 mm), for example, the error would be approximately 0.01%. Smaller gage lengths, such as those used when deriving strain maps, would yield proportionally larger margins of error depending on the gage length.

4. Results

4.1 Cyclic Swell-Shrink Behaviour

As the GCL is hydrated, dried, and subsequently rehydrated, it displays a similar cyclic behavior in its strain response. As the GCL is wet, it swells, resulting in positive strains; following the drying phase, shrinkage across the sample is evident, shown by a negative strain. Figure 4 shows the response of Pan “C” over 40 cycles; results shown are of the absolute maximum transverse strain as measured between the two vertical (longitudinal) grid lines. Although this sample does recover some strain upon rewetting, the overall trend is still toward negative, or increasing shrinkage, strain. This suggests that there is a degree of shrinkage strain that, after several wetting and drying cycles, is unrecoverable. This behavior is consistent with previous pan tests.

Figure 5 shows the strain envelopes for each of the three samples. The strain amplitude, or difference between the swelling and shrinkage curves, increases with the number of cycles. After 40 cycles, the strain amplitude for each test is approximately 6-7%. Although this value is relatively similar between different samples, the absolute maximum strain shows variation, with sample “B” registering less shrinkage than either “A” or “C”. The variation in maximum shrinkage was between -11.1% (sample B, dry mass of 5880 g/m²) and -17.8% (sample A, dry mass of 4820 g/m²); this is likely due to inherent variations in the GCL samples which had significantly different mass per unit area (Table 2) and possibly also the heat-seaming process. By the end of 40 cycles, shrinkage was no longer increasing with the number of cycles, having reached a constant value.

4.2 Location of Maximum Transverse Shrinkage

In previous tests on restrained GCL samples, the maximum strain would have occurred at or near the middle of the sample, as a result of sample necking (Bostwick et al. 2007, 2008). For the tests on heat-seamed GCLs however, the excess material located in the centre portion of the sample prevents the GCL from shrinking preferentially at that point. Instead, the maximum shrinkage tends to occur just at the edge of the seamed portion of the sample, as shown in Figure 6. Although the maximum shrinkage occurred outside of the seamed portion of the sample, the centre section did still experience shrinkage over time (Figure 7). As with the maximum shrinkage, results varied between the three samples. Table 3 shows a comparison between the transverse strains measured at the centre of each sample, and the maximum transverse strains. On average, the centre strain was approximately 80% of the maximum.

4.3 Longitudinal Shrinkage and Change in Seam Position

In previous restrained shrinkage tests on unseamed GCL, the strain in the transverse direction was of primary interest. However, when examining a seamed GCL sample, in which tension is induced longitudinally due to the restraint at both ends, any change occurring at the edge of the heat-tack becomes of interest since that strain will be analogous to the forces that the GCL seam in the field must withstand. It is important to note that only changes in the top seam could be studied. Since the lower seam edge could not be photographed, it was not possible to monitor the strain in the GCL adjacent to the seam using the geoPIV program.

Figure 8 shows Sample “A” after undergoing an increasing number of wetting and drying cycles. Necking in the transverse direction is evident, with the maximum shrinkage occurring, as previously noted, at the edge of the seamed portion (directly above the words “40 cycles” in the image). As the number of cycles increased, a change in the position of the upper (visible) seam edge becomes apparent. This area of the sample was magnified and is shown in Figure 9 at both 0 (pre-test) and 40 cycles with both the grid lines and the seam edge emphasized for greater clarity. To quantify this change at the seam, and to attempt to make a comparison between different samples, an index value of “seam movement” was calculated. Since the lower seam edge was covered, and therefore not observable, the position of the seam edge was compared to a relatively unchanging location on the sample – the topmost horizontal gridline, closest to the clamp. This gage distance is shown in Figure 6.

The strain calculated over this gage distance is shown in Figure 10. As the two measurement locations were in fact moving away from each other, this strain is expressed

as positive (tension). The sample showing the greatest change in the position of the upper seam was Sample “B”, with Sample “A” registering the least. This appears to be inversely correlated to the transverse strains observed, where Sample “B” recorded the smallest strain and “A” the largest (Table 4). Due to the variable nature of the GCL / heat tacking (differing strengths of seams were obtained and it was observed that the width of tacking was not consistent) it is difficult to say whether this observation is causal, or simply coincidental. More tests would be needed to confirm a definite relationship.

It is important to note that, despite the high values of strain adjacent to the seam, the two pieces of GCL joined at heat-tacked seam remained firmly attached.

5. Full Sample Response

The transverse sample strains discussed above, as with those obtained in previous shrinkage tests, were calculated between the two longitudinal grid lines of the sample, resulting in an average strain across the sample. Although this type of analysis gives a good idea of the shrinkage to be expected across a panel, it tends to obscure small details that may occur in different areas of the GCL. To examine the shrinkage throughout the entire sample, 64-pixel patches were created, with a spacing between centers of 64-pixels, as shown in Figure 11. The edge of the seam is also shown and strains were not monitored at the edge of the seam because the reversal of directions for GCL movement at this location makes it impossible to analyze via geoPIV. Strain is calculated between each pair of adjacent patches, in both the transverse and longitudinal directions.

5.1 Displacement-Vector Plots

Examining the displacement vector plots of full panel shrinkage after 40 cycles (Figure 12) shows that for all three samples, shrinkage-induced movement is away from the visible seam edge. The approximate position of this seam edge is noted in the figure by a dashed line. Although the displacement vectors show that there is movement in both halves of the seamed sample, the magnitudes are greater in the lower portion, particularly near the seam.

The displacement vector plot for Sample “B” shows little transverse shrinkage in the lower portion of the figure; instead, much of the movement is in the longitudinal direction. This is consistent with the strain results discussed above where Sample “B” was shown to have the most longitudinal tensile strain (21.5%) and hence displacement over the specified gage length. The vector plot also provides some insight into the movements that were responsible for Sample “B” having the smallest maximum transverse shrinkage (-11.1%). Given the similarity of the samples except for the differences in mass per unit area, the differences in the deformation patterns between the three samples is likely a result of this variation in mass per unit area (which may also occur within the sample) perhaps combined with variability in the heat-tacking process itself.

5.2 Strain Maps

The displacement vectors shown in Figure 12 can be used to generate the local transverse strains which can be presented as a contour plot (Figure 13) referred to as a “strain map”. As with the vector plots, geoPIV was unable to analyze the area directly adjacent to the seam (white area on the figure) .

The strain maps for all three samples show a large variation of strain across the sample, indicating that strain due to GCL shrinkage is not uniform. In addition, the shrinkage patterns appear relatively random; that is, when comparing the shrinkage patterns of each of the different samples, there is no clear trend. This supports the hypothesis that GCL4 is a highly variable material, and that these variations influence the way it shrinks when exposed to wetting and drying cycles (Figure 13). In Sample “C”, for example, the maximum shrinkage after 40 cycles, measured between the two longitudinal border lines, is -15.6%. The method of calculating this strain simply averages the higher and lower strains that occur at this location. When looking at the strain map for sample “C”, we can see that, in the location where the maximum strain of -15.6% occurs, local shrinkage strains range from -4% to -18%; a large range that is not captured when simply looking at the averaged maximum shrinkage.

6. Heat-Tack Strength

Following the completion of the cyclic tests, each of the heat-tacked samples was removed from the corresponding pan, and the residual seam strength tested as per ASTM D4595. In addition, two samples of virgin heat-seamed material (i.e. samples that did not undergo wet-dry cycling) were tested in the same manner. The results are shown in Table 5. The samples failed in three different ways. They were:

- Pre-engineered groove – The sample tore apart through the pre-engineered groove at the roll edge adjacent to the heat-tacked seam;
- Seam – the sample failed through the heat-tacked seam; and
- Geotextile – One or both of the geotextiles adjacent to the seam began to tear, causing the needlepunching to pull apart

The average heat-tacked strength after wet-dry cycling (12.1 kN/m) was at least as high as the average heat-tacked strength of a virgin sample (10.2 kN/m) suggesting that the wet-dry cycling did not weaken the strength of the heat-tacked bond. The difference in results between the two sets of data illustrates the variability of GCL4 and the seam.

Similar strength tests were also carried out on virgin samples of un-seamed GCL4 material; the tests were performed as per ASTM D4595 on both the cross and machine directions, as well as through the pre-engineered groove. The results (Table 6) indicate that the strength of a seamed sample, with forces generated in the cross-roll (longitudinal, in these tests) direction, (ranging from 10.0 to 14.0 kN/m), is similar to the cross-roll strength of an unseamed sample (range from 10.8 to 14.8 kN/m) suggesting that the heat-tack is at least as strong as the GCL itself. This is further evidenced by the fact that the seamed samples failed in three different ways. Of the five seamed samples tested, only 2 failed through the heat-tacked seam.

7. Conclusions

A testing program was initiated to examine the behavior of heat-tacked GCL seams under cyclic wetting and drying. Following the completion of the experiments, at 40 cycles, it was concluded that the transverse shrinkage behavior of heat-seamed samples was similar to that observed in previous shrinkage tests performed on unseamed GCL. However, unlike previous tests, the extra material at the heat-tacked center portion of the sample hindered shrinkage at that location. The samples instead shrank preferentially at the quarter point (the closest point to the centre of sample that does not have heat-tacked seam material).

As the samples shrank in the transverse direction, the visible seam edge began to move. Both the transverse and longitudinal movements appear to have some variation. There did not appear to be any separation of the two GCL pieces at the heat-tacked seam.

Strain maps of the samples show that the GCL shrinkage varies across the sample. There did not appear to be a uniform shrinkage pattern between the 3 samples.

The heat-tacked seam had a strength comparable to the virgin GCL. The strength of the heat-tacked seam subjected to 40 wet-dry cycles was at least as high as that of virgin heat-tacked samples, suggesting that the bond did not weaken during the shrinkage testing. After 40 cycles, the samples remained heat-tacked, suggesting the technique has promise as one method of preventing panel shrinkage.

It is noted that the experiments reported herein were small-scale laboratory tests, under idealized conditions, and that the behavior in the field may differ due to more extreme conditions that may develop in some field applications, as well as a greater amount of material between seams available to shrink in the field. Both factors may induce forces in the GCL and/or heat-tacked GCL seam greater than observed in the present paper. However, it was also shown that the seam was as strong as the GCL adjacent to the seam. Thus, the GCL tested would be as likely (or perhaps more likely) to fail due to forces induced by shrinkage of the GCL as the heat-tacked seam itself.

While heat-tacking appeared to work well in the Carlota Mine application and in the pan shrinkage tests reported in this paper, this does not mean that the approach will work in all applications. For example, the conditions that gave rise to the large panel separations reported by Koerner and Koerner (2005a, b) and Thiel et al. (2006) for the GCL tested could potentially cause a failure either in the seam or the material adjacent to

the seam for this GCL. Thus while heat-tacking may reduce the risk of panel separation it does not alter the need to ideally cover composite liners as quickly as practicable after placement. Until such time as that there is more data to confirm the effectiveness of heat-taking in a variety of field situations, it is recommended that more field research be conducted to establish whether the stresses induced in GCLs with heat tacked seams are sufficient to cause either failure of the seam or tearing of the GCL adjacent to the seam. This is especially important when the GCLs used have been observed to give rise to high shrinkage and panel separation in field applications.

8. Acknowledgements

The study reported herein was financially supported by the Natural Science and Engineering Research Council of Canada (NSERC), the Ontario Centres of Excellence, and Terrafix Geosynthetics Inc. The authors are grateful to their industrial partners, Terrafix Geosynthetics Inc, Solmax International, Ontario Ministry of Environment, Gartner Lee Ltd, AMEC Earth and Environmental, Golder Associates Ltd., and CTT group. The funding for the equipment used, provided by the Canada Foundation for Innovation, the Ontario Innovation Trust and NSERC, is also gratefully acknowledged. The authors also gratefully acknowledge the Carlota Copper Company for providing the samples, CTT group for conducting the strength tests on virgin GCL, and Dr. A. Take for assistance with the geoPIV software. The opinions stated here in are solely those of the authors.

9. References

- ASTM D 4595 Standard Test Method for Tensile Properties of Geotextiles by the Wide-Width Strip Method, *American Society for Testing and Materials*, West Conshohocken, Pennsylvania, USA.
- Bostwick, L.E., Rowe, R.K., Take, W.A. and Brachman, R.W.I. (2007). The effect of sample size on shrinkage of a non scrim reinforced geosynthetic clay liner, *60th Canadian Geotechnical Conference*, Ottawa, ON, 2123-2128.
- Bostwick, L.E., Rowe, R. K, Take, W. A and Brachman, R.W.I. (2008). Observations of the dimensional stability of four GCL products under combined thermal and moisture cycles, *Geoamericas 2008*, Cancun, Mexico, 435-443.
- Bostwick, L.E. (2009). Laboratory study of geosynthetic clay liner shrinkage when subjected to wet/dry cycles, MSc. Thesis, Queen's University, Kingston.
- Brachman, R.W.I. and Gudina, S. (2008). Geomembrane strains from coarse gravel and wrinkles in a GM/GCL composite liner, *Geotextiles and Geomembranes* 26 (6) 488–497.
- Gassner, F. (2009). Field observation of GCL shrinkage at a site in Melbourne Australia, *Geotextiles and Geomembranes*, In Press, doi:10.1016/j.geotexmem.2008.09.010.
- Koerner, R.M. & Koerner, G.R. (2005a). “GRI White Paper #5 - In-situ separation of GCL panels beneath exposed geomembranes”, Geosynthetic Institute, Folsom, PA, April 15, 2005, 21 p.
- Koerner, R.M. & Koerner, G.R. (2005b). In-situ Separation of GCL panels beneath exposed geomembranes, *GFR*, June-July 2005, 34-39.
- Rowe, R. K. (2005). Long-term performance of contaminant barrier systems, *Geotechnique*, 55(9): 631–678.
- Rowe, R.K., Bostwick, L.E. and Thiel, R. (2009). GCL Shrinkage and the potential benefits of heat-tacked GCL seams, *Geosynthetics 2009*, Salt Lake City, UT, USA., 10-18.
- Rowe, R.K., Quigley, R.M., Brachman, R.W.I., and Booker, J.R. (2004). Barrier Systems for Waste Disposal Facilities, Taylor & Francis Books Ltd (E & FN Spon) London, 587p

- Thiel, R. and Thiel, C. (2009). GCL shrinkage - A possible solution, *Geosynthetics*, February/March 2009: 10-21.
- Thiel, R., Giroud, J.P., Erickson, R., Criley, K. and Bryk, J. (2006). Laboratory measurements of GCL shrinkage under cyclic changes in temperature and hydration conditions, *8th International Conference on Geosynthetics*, Yokohama, Japan 1: 21-44.
- Thiel, R. and Richardson, G. (2005). Concern for GCL shrinkage when installed on slopes, *JGRI-18 at GeoFrontiers*, GII Publications, Folsom, PA, USA, paper 2.31.
- White, D.J., Take, W.A., and Bolton, M.D. (2003). Soil deformation measurement using particle image velocimetry (PIV) and photogrammetry, *Geotechnique* 53 (7): 619-63.

Table 1 - Properties of some needlepunched GCLs tested by both Thiel et al. (2006) and Bostwick (2009)

Product	Cover GT*	Carrier GT*	Bentonite granularity	Thermally treated	Maximum Shrinkage Thiel et al (2006) (%) [†]	Maximum Shrinkage Bostwick (2009) (%)	Maximum separation observed in field** (mm)
GCL1	NW	W-T	Fine	Yes	-14.5	-10.4	-
GCL2	NW	NWSR-T	Fine	Yes	-12.9	-10.8	-
GCL3	NW	W	Coarse	No	-20.6	-11.6	300
GCL4	NW	NW	Coarse	No	-23.0	-14.4	1200

* NW=nonwoven, W=woven, NWSR = Scrim reinforced nonwoven, T = thermally treated, ** as reported by Thiel et al. (2006)

[†] Sign convention adopted herein: negative strain denotes shrinkage

Table 2 - Initial Properties of GCL Specimens

Test	Initial W/C (%)	Water Added (g)	Target W/C (First Cycle) (%)	Target W/C (Subsequent Cycles) (%)	Dry mass per unit area (g/m ²)
A	5.8	255	65.9	61.1	4490
B	6.6	333	66.5	61.0	5880
C	6.4	274	66.5	61.1	4820

Table 3 - Maximum and centre transverse shrinkage strain

Sample	Maximum shrinkage strain (%)	Shrinkage strain at centre (%)	Ratio of Centre to Maximum
"A"	-17.8	-13.8	0.78
"B"	-11.1	-9.8	0.88
"C"	-15.6	-11.6	0.74

Table 4 - Maximum transverse shrinkage strain and longitudinal tensile strain in GCL adjacent to seam

Sample	Maximum Shrinkage Strain (%)	Maximum Tensile strain in GCL adjacent to seam
"A"	-17.8	11.8
"B"	-11.1	21.2
"C"	-15.6	17.2

Table 5 - Strength Properties of Heat-Seamed GCL

	Test	Method of Failure	Strength (kN/m)	Average Strength (kN)
Wet-Dry Cycled	“A”	Pre-engineered Groove	14.0	12.1
	“B”	Seam	10.0	
	“C”	Geotextile	12.2	
Virgin	1	Pre-engineered Groove	10.2	10.2
	2	Seam	10.2	

Table 6 - Properties of Virgin (Non-Heat Seamed) NW/NW GCL

Test	Breaking Strength (kN/m)	Average Breaking Strength (kN/m)	Std Dev
Roll Direction	6.2	8.0	1.5
	7.4		
	8.2		
	7.8		
	10.8		
	7.7		
Cross Direction	12.4	12.7	1.4
	11.5		
	13.2		
	14.8		
	10.8		
	13.2		
Pre-Engineered Groove	8.0	8.5	2.8
	8.3		
	8.0		
	6.5		
	6.1		
	13.9		



Figure 1 - Heat-tacking GCL panels with a 150 mm overlap to form a seam.

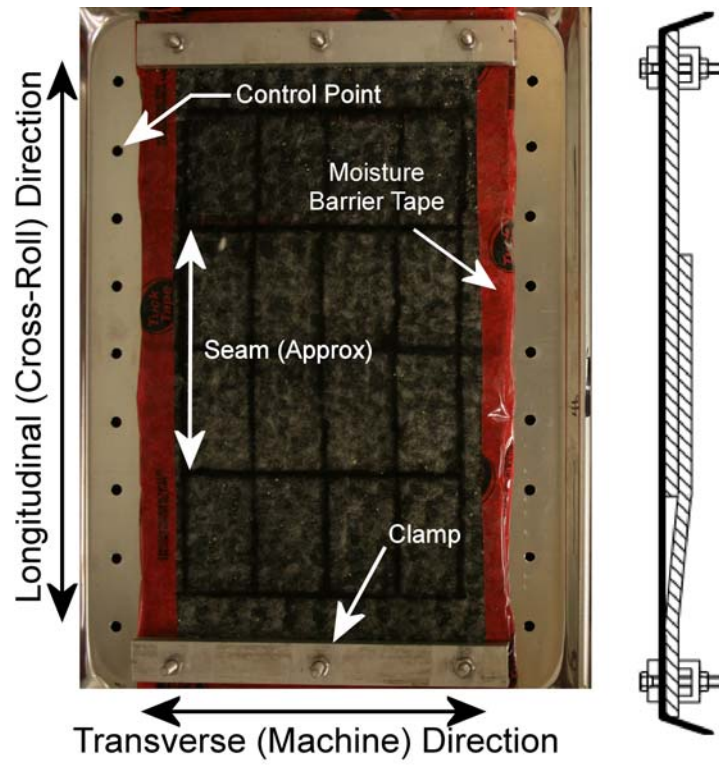


Figure 2 - Initial specimen setup

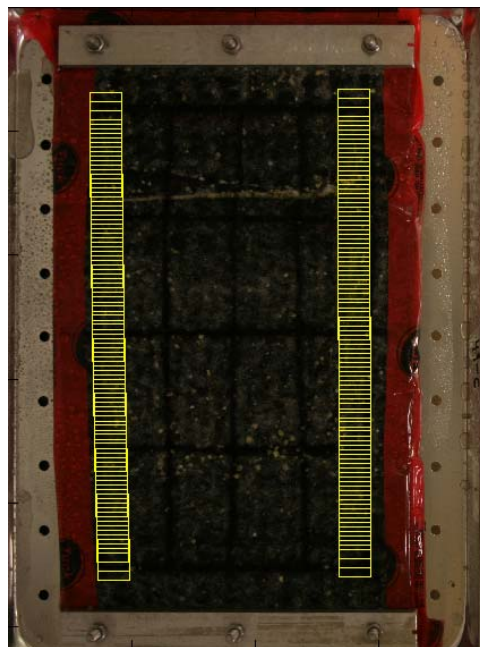


Figure 3 - Virtual patches used to calculate transverse shrinkage

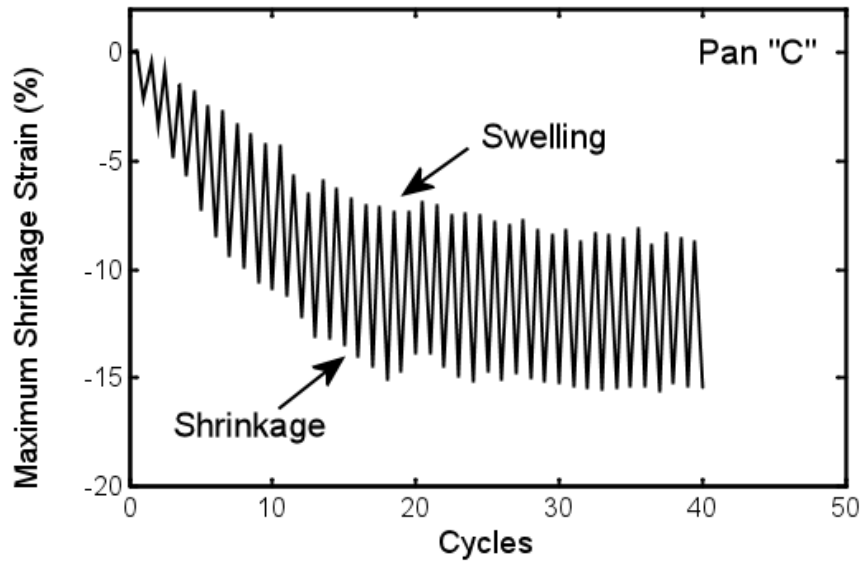


Figure 4 - Transverse shrink-swell behaviour at location of maximum shrinkage (Pan C)

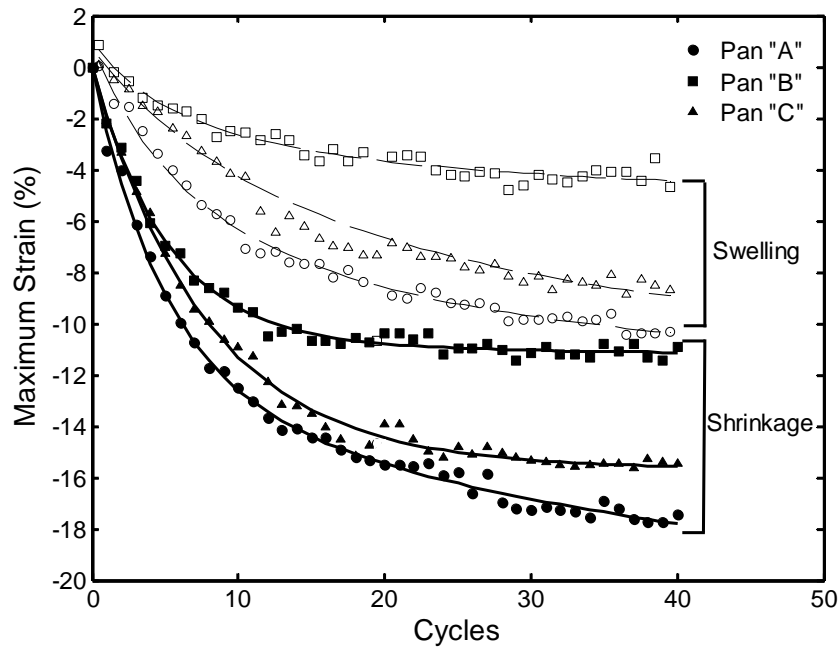


Figure 5 - Transverse shrinkage and swelling envelopes at location of maximum shrinkage for all 3 specimens

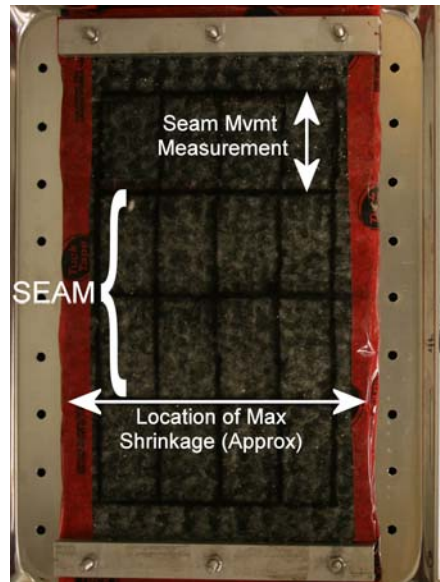


Figure 6 - Key shrinkage locations

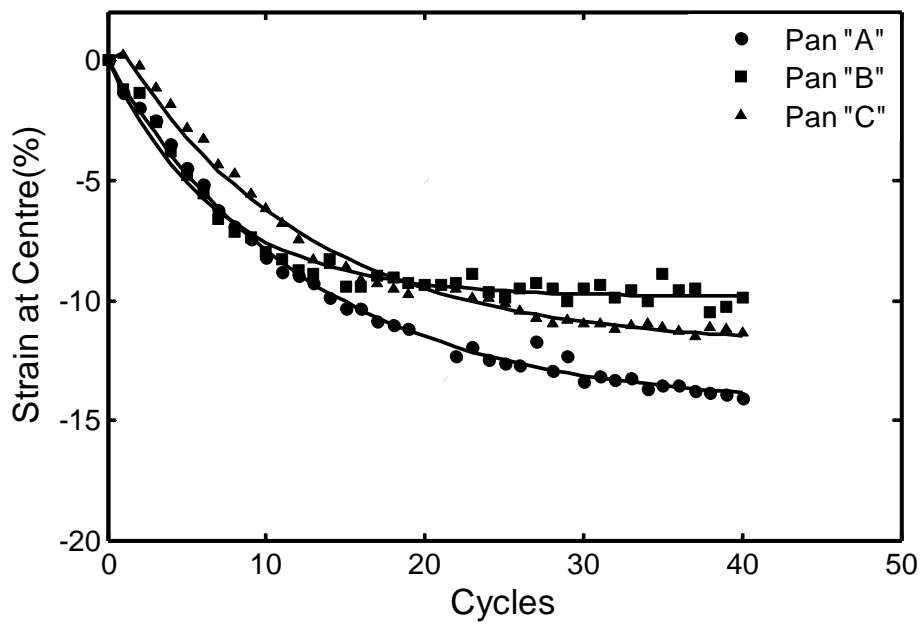


Figure 7 - Transverse shrinkage at centre of specimen (at seam)

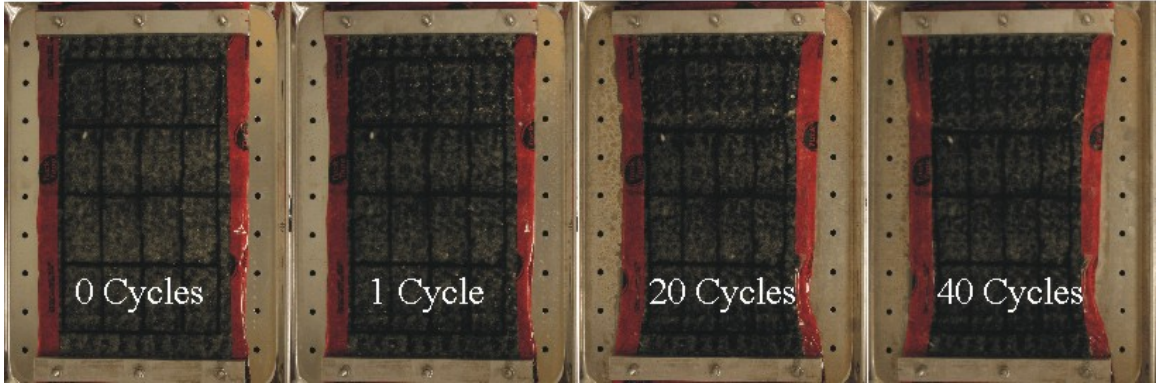


Figure 8 - Shrinkage of Pan A over time

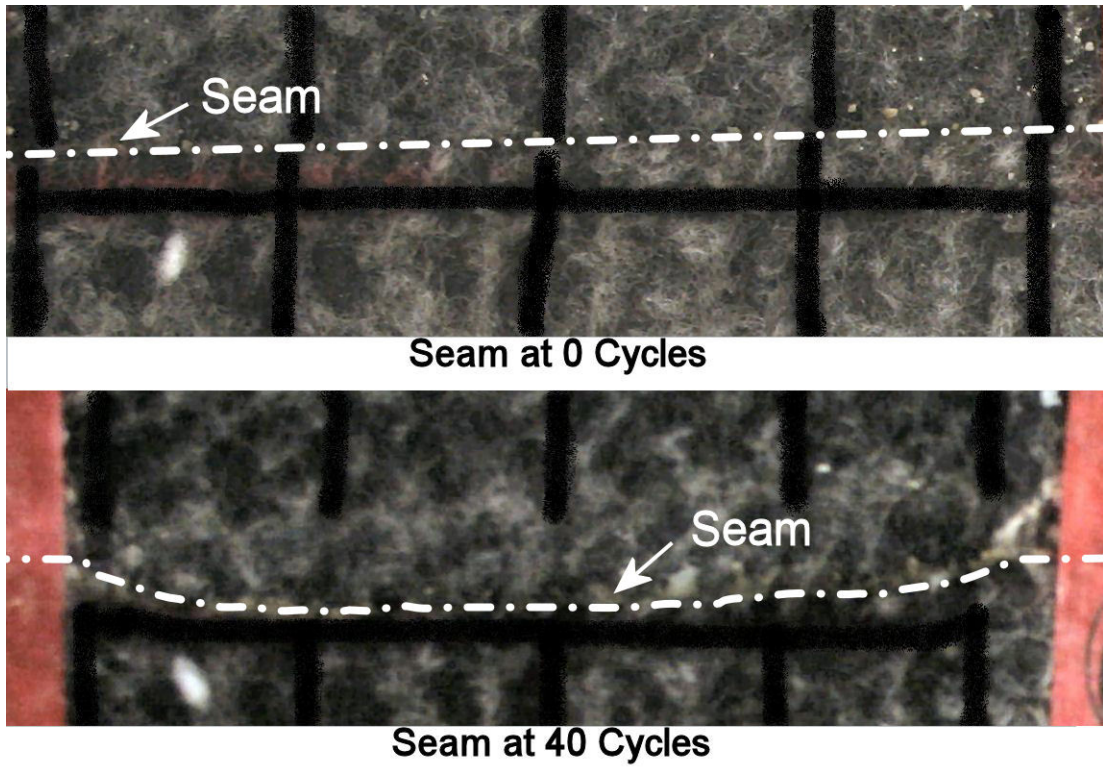


Figure 9 - Movement of edge of seam due to shrinkage (Pan A)

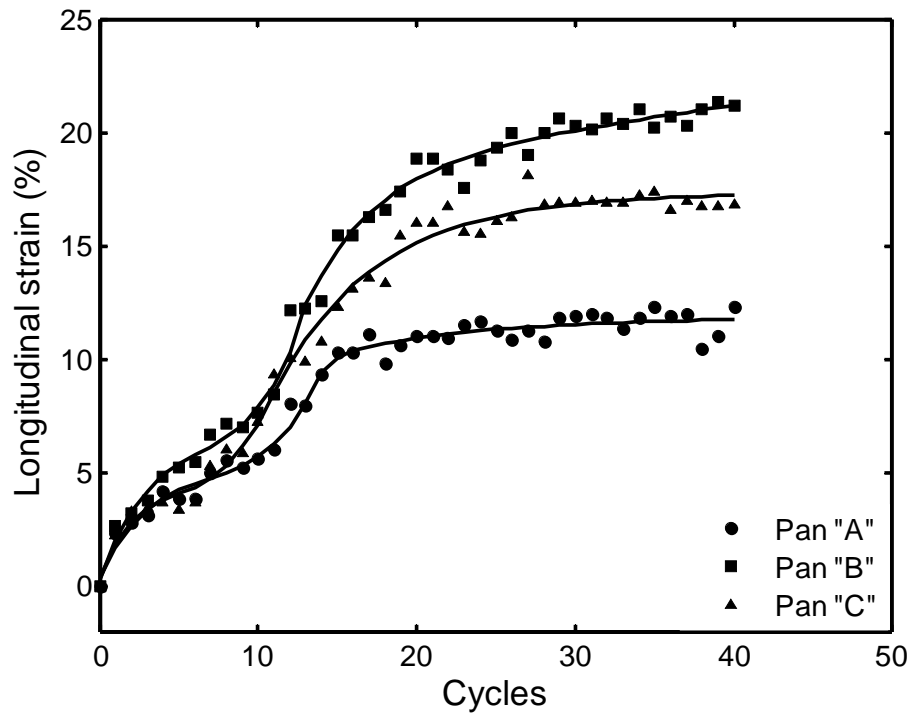


Figure 10 - Longitudinal tensile strain in GCL adjacent to the seam

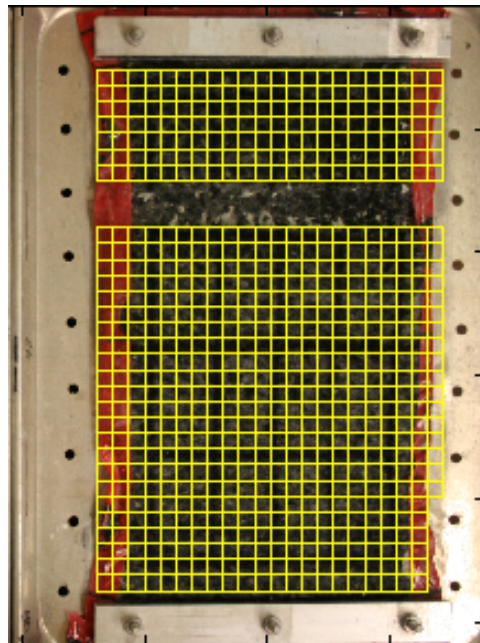


Figure 11 - Virtual patches used to track movement across full specimen

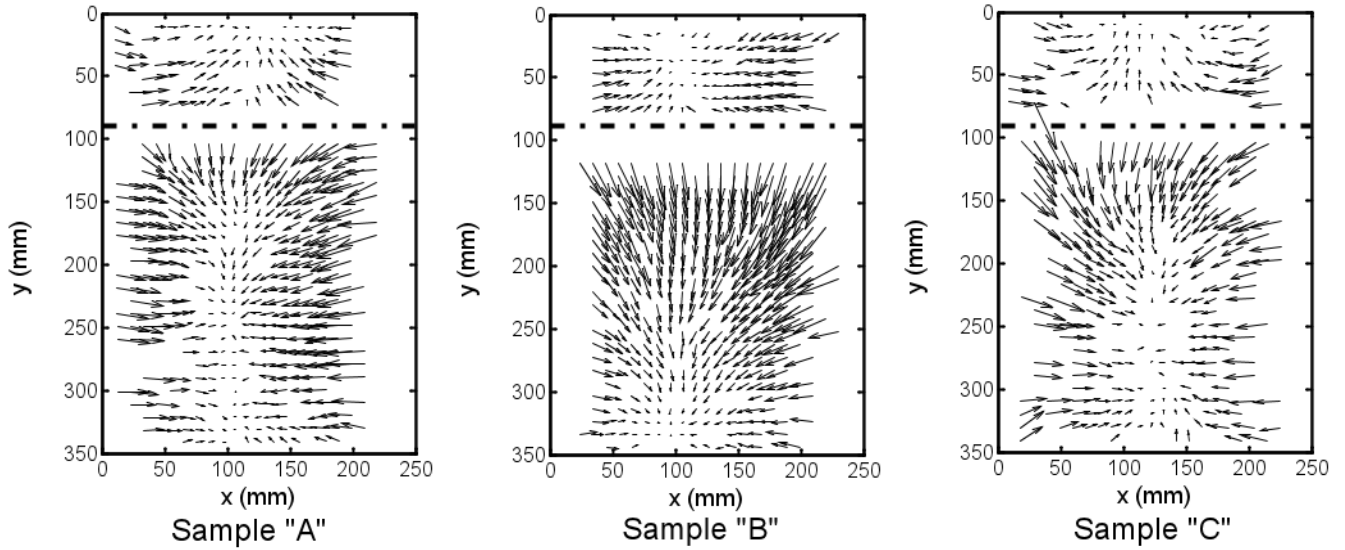


Figure 12 - Vector plots at 40 Cycles (position of this seam edge is shown by the dashed line)

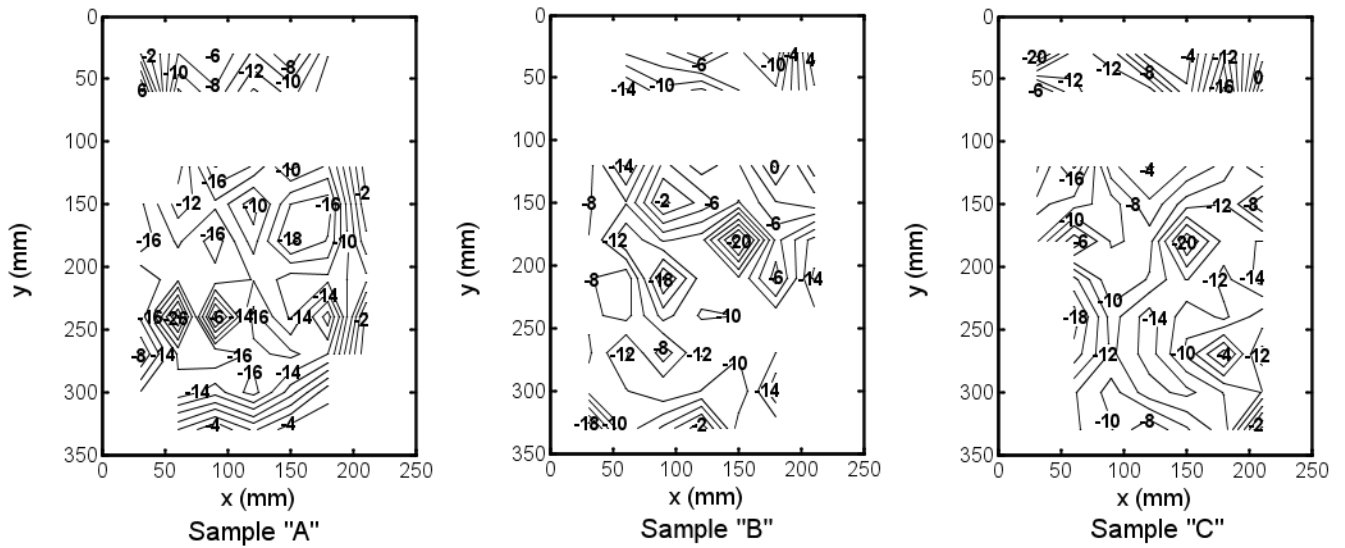


Figure 13 - Transverse strain (%) maps